Eur. Phys. J. B **4**, 185–190 (1998)

THE EUROPEAN PHYSICAL JOURNAL B

Steady-state populations of a driven three-level atom in a broad-band squeezed vacuum

Z.-C. Wang[1,2], Z.-Y. Chen[2,a], and Y. Xu[2]

[1] CCAST (World Laboratory), P.O. Box 8730, Beijing 100080, P.R. China
[2] Department of Physics, Lanzhou University, Lanzhou 730000, P.R. China

Received: 28 May 1997 / Revised and Accepted: 10 December 1997

Abstract. A theoretical study is made of the steady-state populations of a three-level atom in a ladder configuration, driven by a superposition of a monochromatic laser wave with a broad-band squeezed vacuum. The master equation for the system and the atomic Bloch equations are derived. The steady-state populations are calculated numerically and shown graphically as functions of two-photon detuning for various cases of the squeezed vacuum. It is shown that, the atomic populations depend strongly on the relative phase of the driving field and the squeezed vacuum. When the phase matching condition is fulfilled, there will be a strong two-photon resonant absorption from the squeezed vacuum, a characteristic different from absorption of photons from a classical field.

PACS. 42.50.Dv Nonclassical field states; squeezed, antibunched, and sub-Poissonian states; operational definitions of the phase of the field; phase measurements

1 Introduction

Since the first successful generation of squeezed light [1] about a decade ago, the interaction of squeezed light with atomic systems has attracted considerable interest. As first predicted by Gardiner [2], the squeezed vacuum can inhibit decay of one of the atomic polarization quadratures of a two-level atom. This modification opens the possibility of obtaining subnatural line widths in resonance fluorescence [3] and in the weak-field atomic absorption spectrum [4]. A variety of other effects emphasizing the novel features of the interaction between two-level atoms and the squeezed vacuum have also been predicted. Examples include squeezing induced transparency [5], level shifts [6], asymmetric and dispersive profiles in fluorescence spectra [7] and amplification without population inversion [8]. The effects of finite-bandwidth squeezed light on the fluorescence and absorption spectra are also studied [9]. To date, these predictions have not been experimentally tested.

The effects of a broad-band squeezed vacuum on three-level atoms have also been investigated [10–13]. In a three-level atom in lambda, vee and ladder configurations interacting with a squeezed vacuum field, there are spectacular qualitative changes in the steady-state populations relative to the ordinary vacuum, including two-photon population inversion [10–12]. Futher work has also been done to study the effect of a broad-band squeezed vacuum on the resonance fluorescence from three-level atoms [14–16]. In particular, Ferguson *et al.* [14] have investigated how a narrow-band squeezed vacuum field coupled to one of the two atomic transitions affects the fluorescence emitted from the other transition.

Recently, great attention has been paid to the effect of a squeezed vacuum on the two-photon excitation rate for a three-level atom in the ladder configuration [17], where a linear dependence of the excitation rate on the excitation intensity in the weak field limit is predicted, instead of a quadratic one for classical excitation field [18]. In particular, an experiment has already been performed on the squeezing-modified two-photon absorption in atomic cesium where fundamental alternation of atomic radiative processes by the nonclassical field has been demonstrated [19].

In this paper, we will examine the effect of superposition of coherent light with a broad-band squeezed vacuum on the steady-state populations of a three-level atom in a ladder configuration. We assume that three atomic levels are nearly equispaced and the atom is driven by a single monochromatic coherent field coupled to the two possible atomic transitions. We assume moreover that the bandwidth of the squeezed vacuum is much larger than both the natural linewidth of the transitions and the difference between the frequencies of the two atomic transitions. Thus a single broad-band squeezed vacuum is coupled to both transitions. It leads to interesting differences between the previous study [16] and the present one. In the previous study [16], the three-level atom is assumed to be driven by two monochromatic fields and interacting with two statistically independent broad-band squeezed

[a] e-mail: xinghz@lzu.edu.cn

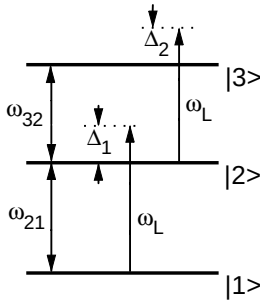

Fig. 1. Three-level atom in a ladder configuration with nearly equal transition frequencies driven by a single coherent laser field of frequency ω_L detuned from the atomic transition frequencies by $\Delta_1 = \omega_L - \omega_{21}$ and $\Delta_2 = \omega_L - \omega_{32}$.

baths. As a result, the two-photon correlation terms are excluded in the master equation and the optical Bloch equations therein. Secondly, the steady-state populations are treated as measures of photon absorption probability and shown as functions of two-photon detuning in the present paper, while the variation of the steady-state populations *versus* the amplitude of the resonant driving fields is interested therein [16]. Noting that the effect of including a cavity into the configuration is merely to degrade the strength of the two-photon correlation of the squeezed vacuum without altering the essential features [10,20,21], we will consider likewise a free-space squeezed vacuum for simplicity.

The paper is organized as follows. In Section 2, the model is described, and the master equation and the optical Bloch equations are derived. In Section 3, the steady-state atomic populations are calculated numerically and shown graphically as functions of two-photon detuning for various cases of the squeezed vacuum. A brief summary is included in Section 4.

2 Master equation and Bloch equations

Consider a three-level atom in a ladder configuration with states $|1\rangle$, $|2\rangle$ and $|3\rangle$ having nearly equispaced energies E_1, E_2 and E_3 respectively ($E_3 > E_2 > E_1$). The atom is driven by one linearly polarized monochromatic coherent field of frequency ω_L coupled to both the 1-2 and 2-3 transitions and is furthermore coupled to all other modes of the electromagnetic field which are assumed to be in a broad-band squeezed vacuum state (Fig. 1). The atomic transition frequencies between the ground state $|1\rangle$ and the intermediate state $|2\rangle$, and between the intermediate state $|2\rangle$ and the upper state $|3\rangle$ are respectively ω_{21} and ω_{32}, where $\hbar\omega_{ij} = E_i - E_j$. These transitions are associated with electric dipole matrix elements μ_{12} and μ_{23} (assumed real for simplicity) respectively, whereas the 1-3 transition is forbidden in the electric dipole approximation ($\mu_{13} = 0$). In the electric dipole and rotating-wave approximations the Hamiltonian of the system has the following form:

$$H = H_S + H_R + H_{RS} \tag{1}$$

where

$$H_S = H_{SO} + H_I \tag{2}$$

is the system (atom + driving field) Hamiltonian, with

$$H_{SO}|i\rangle = E_i|i\rangle, i = 1, 2, 3, \tag{3}$$

and H_I is the atom–driving field interaction Hamiltonian given as follows,

$$\begin{aligned} H_I = &-\tfrac{1}{2}i\hbar\Omega_1\{|2\rangle\langle 1|\exp\left[-i\left(\omega_L t - \varphi_L\right)\right] \\ &-|1\rangle\langle 2|\exp\left[i\left(\omega_L t - \varphi_L\right)\right]\} \\ &-\tfrac{1}{2}i\hbar\Omega_2\{|3\rangle\langle 2|\exp\left[-i\left(\omega_L t - \varphi_L\right)\right] \\ &-|2\rangle\langle 3|\exp\left[i\left(\omega_L t - \varphi_L\right)\right]\} \end{aligned} \tag{4}$$

where $\Omega_1 = \mu_{12}E_0/\hbar$ and $\Omega_2 = \mu_{23}E_0/\hbar$ are the Rabi frequencies, with E_0 the amplitude and φ_L the phase of the coherent field.

H_R is the Hamiltonian of the quantized electromagnetic field of the squeezed vacuum:

$$H_R = \hbar\sum_\lambda \omega_\lambda \left(a_\lambda^+ a_\lambda + \frac{1}{2}\right) \tag{5}$$

where a_λ and a_λ^+ are the bosonic operators for the field. H_{RS} is the system-squeezed vacuum coupling Hamiltonian in the rotating-wave approximation given as follows:

$$\begin{aligned} H_{RS} = &-\tfrac{i\hbar}{2}\sum_\lambda(\Omega_\lambda^{(1)}a_\lambda|2\rangle\langle 1| - |1\rangle\langle 2|(\Omega_\lambda^{(1)})^* a_\lambda^+) \\ &-\tfrac{i\hbar}{2}\sum_\lambda(\Omega_\lambda^{(2)}a_\lambda|3\rangle\langle 2| - |2\rangle\langle 3|(\Omega_\lambda^{(2)})^* a_\lambda^+) \end{aligned} \tag{6}$$

where

$$\Omega_\lambda^{(1)} = (\mu_{12}\,\hat{e}_\lambda)\left(\frac{2\omega_\lambda}{\hbar\varepsilon_0 V}\right)^{1/2} \tag{7}$$

and

$$\Omega_\lambda^{(2)} = (\mu_{23}\,\hat{e}_\lambda)\left(\frac{2\omega_\lambda}{\hbar\varepsilon_0 V}\right)^{1/2} \tag{8}$$

are the usual one-photon Rabi frequencies of the vacuum field, $\hat{e}_\lambda$ is the unit polarization vector, and $\lambda \equiv (\mathbf{k}, \mathbf{s})$ labels both the propagation vector $\mathbf{k}$ and the polarization $\mathbf{s}$.

A broad-band squeezed vacuum can be generally illustrated by parameters ω_s, $N(\omega_\lambda)$ and $M(\omega_\lambda)$, where ω_s is the carrier frequency of the squeezed vacuum and $N(\omega_\lambda)$ and $M(\omega_\lambda)$ are given in the following expressions:

$$\begin{aligned} \left\langle a_\lambda a_\mu^+\right\rangle &= N(\omega_\lambda) + 1 \text{ for } \omega_\lambda = \omega_\mu, \\ \left\langle a_\lambda^+ a_\mu\right\rangle &= N(\omega_\lambda) \quad \text{for } \omega_\lambda = \omega_\mu, \\ \left\langle a_\lambda a_\mu\right\rangle &= M(\omega_\lambda) \quad \text{for } \omega_\lambda + \omega_\mu = 2\omega_s, \\ \left\langle a_\lambda^+ a_\mu^+\right\rangle &= M^*(\omega_\lambda) \quad \text{for } \omega_\lambda + \omega_\mu = 2\omega_s, \end{aligned} \tag{9}$$

with $|M(\omega_\lambda)|^2 \leq N(\omega_\lambda)\left[N(\omega_\lambda) + 1\right]$, where the equality holds for minimum-uncertainty states. The parameter

$N(\omega_\lambda)$ is the mean photon number of the mode λ in the broad-band squeezed vacuum and the complex parameter $M(\omega_\lambda) = M(2\omega_s - \omega_\lambda) = |M(\omega_\lambda)| \exp(i\varphi_s)$ characterizes the correlations between the field modes at frequency ω_λ and at frequency $2\omega_s - \omega_\lambda$, where φ_s is the phase of the squeezed vacuum. In this paper, we shall suppress the functional dependence of N and M on ω_λ for simplicity.

In the Schrödinger picture, the master equation for the density operator ρ, based on the Born-Markoff approximations [23,24] together with the electric dipole and rotating-wave approximations, is given by

$$\begin{aligned}\frac{\partial}{\partial t}\rho = & -\tfrac{i}{\hbar}\left[H_S, \rho\right] \\ & +\tfrac{1}{2}\left(N+1\right)\sum_{i,j}\Gamma_{ij}\left(\left[S_i^-, \rho S_j^+\right] + \left[S_i^-\rho, S_j^+\right]\right) \\ & +\tfrac{1}{2}N\sum_{i,j}\Gamma_{ij}\left(\left[S_i^+, \rho S_j^-\right] + \left[S_i^+\rho, S_j^-\right]\right) \\ & -\tfrac{1}{2}M\sum_{i,j}\Gamma_{ij}\left(\left[S_i^+, \rho S_j^+\right] + \left[S_i^+\rho, S_j^+\right]\right)\exp(-2i\omega_s t) \\ & -\tfrac{1}{2}M^*\sum_{i,j}\Gamma_{ij}\left(\left[S_i^-, \rho S_j^-\right] + \left[S_i^-\rho, S_j^-\right]\right)\exp(2i\omega_s t)\end{aligned} \tag{10}$$

where $S_1^+ = |2\rangle\langle 1|$, $S_2^+ = |3\rangle\langle 2|$, $S_1^- = |1\rangle\langle 2|$, and $S_2^- = |2\rangle\langle 3|$. The sum over i, j is with 1, 2 only. Here we have already neglected the intensity dependent Lamb shifts and the corresponding frequency shift in M [10,13]. The parameters Γ_{11} and Γ_{22} are the rates for spontaneous emissions from state $|2\rangle$ to state $|1\rangle$ and from state $|3\rangle$ to state $|2\rangle$, respectively. Γ_{21} and Γ_{12} are the coherence transfer rates which couple to the 1-2 and 2-3 atomic coherences:

$$\Gamma_{21} = \Gamma_{12} = \frac{\mu_{12}\mu_{23}}{6\pi\varepsilon_0\hbar c^3}\left(\omega_{21}^3 + \omega_{32}^3\right). \tag{11}$$

When μ_{12} and μ_{23} are orthogonal, Γ_{12} is zero. Evaluation of Γ_{12} produces the following selection rules in terms of angular momentum quantum numbers: $\mathbf{J}_2 - \mathbf{J}_1 = \pm 1, 0$, $\mathbf{J}_2 - \mathbf{J}_3 = \pm 1, 0$, and $\mathbf{M}_2 - \mathbf{M}_1 = \mathbf{M}_2 - \mathbf{M}_3 = \pm 1, 0$. In this paper, we set Γ_{21} to $(\Gamma_{11}\Gamma_{22})^{1/2}$.

From the atomic master equation (10), we can obtain the Bloch equations for the atomic density matrix elements. We define ρ_{ij} as $\langle i|\rho|j\rangle$, where i, $j = 1, 2, 3$. The matrix elements of ρ according to equation (10) satisfy linearly coupled equations of motion containing explicit time-dependent factors of the complex exponential type. These can be removed by using the following transformations:

$$\begin{aligned}\sigma_{ii} &= \rho_{ii}\ , \quad i = 1, 2, 3, \\ \sigma_{12} &= \rho_{12}\exp[-i(\omega_L t - \varphi_L)] = \sigma_{21}^*, \\ \sigma_{23} &= \rho_{23}\exp[-i(\omega_L t - \varphi_L)] = \sigma_{32}^*, \\ \sigma_{13} &= \rho_{13}\exp[-2i(\omega_L t - \varphi_L)] = \sigma_{31}^*.\end{aligned} \tag{12}$$

In terms of the σ_{ij}, the Bloch equations can be written in simple form using the following suitable scaled variables:

$$\begin{aligned}\tau &= \left(\Gamma_{11} + \Gamma_{22}\right)t, \gamma_1 &&= \Gamma_{11}/\left(\Gamma_{11} + \Gamma_{22}\right), \\ \gamma_2 &= \Gamma_{22}/\left(\Gamma_{11} + \Gamma_{22}\right), \gamma_{21} &&= \Gamma_{21}/\left(\Gamma_{11} + \Gamma_{22}\right), \\ \xi_1 &= \Omega_1/\left(\Gamma_{11} + \Gamma_{22}\right), \xi_2 &&= \Omega_2/\left(\Gamma_{11} + \Gamma_{22}\right), \\ \Delta &= \left(\Delta_1 + \Delta_2\right)/\left(\Gamma_{11} + \Gamma_{22}\right), \delta &&= \left(\Delta_2 - \Delta_1\right)/\left(\Gamma_{11} + \Gamma_{22}\right).\end{aligned} \tag{13}$$

Thus τ is the scaled time, γ_1 and γ_2 scaled relaxation rates, γ_{21} scaled coherence transfer rate, ξ_1 and ξ_2 scaled Rabi frequencies, Δ is the scaled two-photon detuning and δ the difference between the scaled one-photon detunings. Furthermore, we define $\Delta_s = 2\left(\omega_s - \omega_L\right)/\left(\Gamma_{11} + \Gamma_{22}\right)$ which is equal to twice the scaled difference between the carrier frequency of the squeezed vacuum and the frequency of the external laser field. An important quantity arising in the following analysis is the phase $\Phi = 2\varphi_L - \varphi_s$ which is equal to the difference between twice the laser phase and the phase of the squeezed vacuum.
The Bloch equations are as follows:

$$\begin{aligned}\tfrac{\partial}{\partial\tau}\sigma_{11} = & \tfrac{1}{2}\xi_1\left(\sigma_{12} + \sigma_{21}\right) + \gamma_1\left[\left(N+1\right)\sigma_{22} - N\sigma_{11}\right] \\ & +\tfrac{1}{2}\gamma_{21}|M|(\sigma_{13}\exp\left(-i\Delta_s\tau - i\Phi\right) \\ & +\sigma_{31}\exp\left(i\Delta_s\tau + i\Phi\right)), \\ \tfrac{\partial}{\partial\tau}\sigma_{22} = & -\tfrac{1}{2}\xi_1\left(\sigma_{12} + \sigma_{21}\right) + \tfrac{1}{2}\xi_2\left(\sigma_{23} + \sigma_{32}\right) \\ & +\gamma_2\left[\left(N+1\right)\sigma_{33} - N\sigma_{22}\right] \\ & -\gamma_1\left[\left(N+1\right)\sigma_{22} - N\sigma_{11}\right] \\ & -\gamma_{21}|M|(\sigma_{13}\exp\left(-i\Delta_s\tau - i\Phi\right) \\ & +\sigma_{31}\exp\left(i\Delta_s\tau + i\Phi\right)), \\ \tfrac{\partial}{\partial\tau}\sigma_{33} = & -\tfrac{1}{2}\xi_2\left(\sigma_{23} + \sigma_{32}\right) - \gamma_2\left[\left(N+1\right)\sigma_{33} - N\sigma_{22}\right] \\ & +\tfrac{1}{2}\gamma_{21}|M|(\sigma_{13}\exp\left(-i\Delta_s\tau - i\Phi\right) \\ & +\sigma_{31}\exp\left(i\Delta_s\tau + i\Phi\right)), \\ \tfrac{\partial}{\partial\tau}\sigma_{13} = & -\tfrac{1}{2}\left[2i\Delta + \gamma_2\left(N+1\right) + \gamma_1 N\right]\sigma_{13} \\ & +\tfrac{1}{2}\xi_1\sigma_{23} - \tfrac{1}{2}\xi_2\sigma_{12} \\ & -\tfrac{1}{2}\gamma_{21}|M|\left(2\sigma_{22} - \sigma_{11} - \sigma_{33}\right)\ \exp\left(i\Delta_s\tau + i\Phi\right), \\ \tfrac{\partial}{\partial\tau}\sigma_{12} = & -\tfrac{1}{2}\left[i(\Delta - \delta) + \gamma_1\left(2N+1\right) + \gamma_2 N\right]\sigma_{12} \\ & +\tfrac{1}{2}\xi_2\sigma_{13} + \gamma_{21}(N+1)\sigma_{23} \\ & +\tfrac{1}{2}\xi_1\left(\sigma_{22} - \sigma_{11}\right) \\ & -(\gamma_1\sigma_{21} - \tfrac{1}{2}\gamma_{21}\sigma_{32})|M|\exp\left(i\Delta_s\tau + i\Phi\right), \\ \tfrac{\partial}{\partial\tau}\sigma_{23} = & -\tfrac{1}{2}\left[i(\Delta + \delta) + \gamma_1\left(N+1\right) + \gamma_2(2N+1)\right]\sigma_{23} \\ & -\tfrac{1}{2}\xi_1\sigma_{13} + \gamma_{21}N\sigma_{12} + \tfrac{1}{2}\xi_2(\sigma_{33} - \sigma_{22}) \\ & -(\gamma_2\sigma_{32} - \tfrac{1}{2}\gamma_{21}\sigma_{21})|M|\exp\left(i\Delta_s\tau + i\Phi\right).\end{aligned} \tag{14}$$

The equations for σ_{32}, σ_{21} and σ_{31} can be obtained from equations (14) by complex conjugation. In general the optical Bloch equations have oscillating coefficients, here we only consider the case that the frequency of the driving laser is equal to the carrier frequency of the squeezed vacuum. When $\Delta_s = 0$, the coefficients of the equations (14)

become time-independent and steady-state solutions can be obtained. By setting the left-hand side of equations (14) to zero and using $\sigma_{11}+\sigma_{22}+\sigma_{33}=1$ and matrix inversion techniques, we obtain numerical steady-state solutions of equations (14).

3 Steady-state populations of the atomic system

We now focus on the steady-state populations in the upper state $|3\rangle$ and the intermediate state $|2\rangle$ for various cases of the broad-band squeezed vacuum coupled to the atomic system.

The stationary populations σ_{33} and σ_{22} of the atom in ordinary vacuum are well studied in [22], a brief description is included below for convenience of presentation. When the driving field is weak (*e.g.* $\xi=0.2$), σ_{33} has a peak at $\Delta=0$ (zero two-photon detuning) because of simultaneous absorption of two photons from the driving field and a weak resonance at $\Delta=\delta$ (zero lower transition detuning) because of a stepwise excitation to the upper state, and σ_{22} has a one-photon resonance at $\Delta=\delta$. When the driving field is intermediate (*e.g.* $\xi=2$), σ_{33} has a strong two-photon resonance at $\Delta=0$ and a weak resonance at $\Delta=\delta$ which is obscured by power brodening, and σ_{22} has in addition a resonance at $\Delta=0$, due to spontaneous emission from the upper level to the intermediate level following the resonant two-photon absorption.

When $N>0$ and $|M|=0$ the reservoir resembles a thermal bath, with the temperature T given by the Planck formula $N(\omega_\lambda)=[\exp(\hbar\omega_\lambda/(kT))-1]^{-1}$. The populations of the upper state and the intermediate state *versus* two-photon detuning Δ for different N are plotted in Figure 2. It is seen that the results for $N>0$ are dramatically different from that for $N=0$. The existence of photons in the thermal reservoir brings about stimulated emission and absorption processes in the entire range, in addition to spontaneous emission processes. As a result, there is a background in the atomic populations. The height of the background is determined by the Boltzmann distribution:

$$\sigma_{33}/\sigma_{22}=\exp[-\hbar\omega_{32}/(kT)],\ \sigma_{22}/\sigma_{11}=\exp[-\hbar\omega_{21}/(kT)]$$

with $\sigma_{33}+\sigma_{22}+\sigma_{11}=1$. In the range where Δ is sufficiently small, the effect of the driving field combines. When N is not too large (*e.g.* $N=1$), besides the similar resonances already described, σ_{33} exhibits a hill and σ_{22} a dip at $\Delta=-\delta$ (zero upper transition detuning), indicating one-photon transition from state $|2\rangle$ to state $|3\rangle$. When N is sufficiently large (*e.g.* $N=10$), the effect of the driving field is overwhelmed, and a straight line is displayed as in Figure 2. A similar graph applies to the case of a weak driving field such as $\xi=0.2$, with the effect of the driving field overwhelmed at a lower N, and is not shown.

In a squeezed vacuum with nonzero N and $|M|$, the atomic populations depend strongly on the relative phase of the driving field and the squeezed vacuum, namely $\Phi=2\varphi_L-\varphi_s$, as well as on other parameters of the

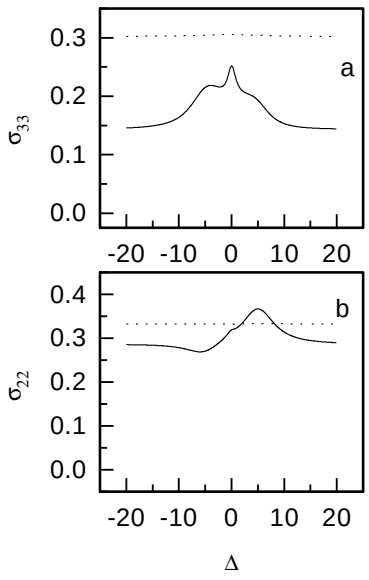

Fig. 2. (a) The steady-state population σ_{33} of state $|3\rangle$ *versus* two-photon detuning Δ. (b) The steady-state population σ_{22} of state $|2\rangle$ *versus* two-photon detuning Δ. Parameter values: $\delta=5$, $\xi_1=\xi_2=\xi=2$, $\gamma_1=\gamma_2=\gamma_{21}=0.5$, $|M|=0$, and different N: 1 (solid line), and 10 (dotted line).

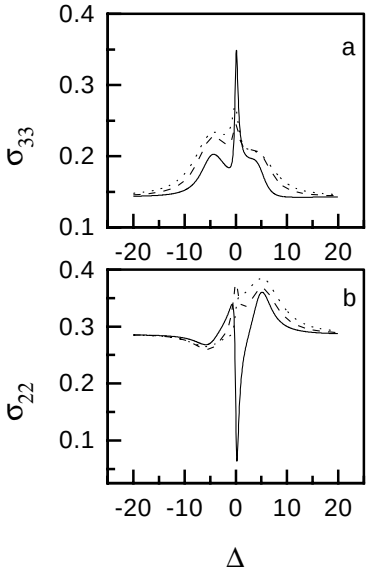

Fig. 3. (a) The steady-state population σ_{33} of state $|3\rangle$ *versus* two-photon detuning Δ. (b) The steady-state population σ_{22} of state $|2\rangle$ *versus* two-photon detuning Δ. Parameter values: $N=1$, $|M|=\sqrt{N(N+1)}$, $\delta=5$, $\xi_1=\xi_2=\xi=2$, $\gamma_1=\gamma_2=\gamma_{21}=0.5$ and different Φ : 0 (solid line), $\frac{\pi}{2}$ (dashed line), π (dotted line).

squeezed vacuum. We plot in Figures 3 and 4 the populations σ_{33} and σ_{22} *versus* two-photon detuning Δ for various Φ with $N=1$ and $N=10$ respectively and $|M|^2=N(N+1)$, *i.e.* the squeezed vacuum in a minimum uncertainty state. It is seen in Figure 3 that, in addition to features already discussed, σ_{33} (σ_{22}) has an upward

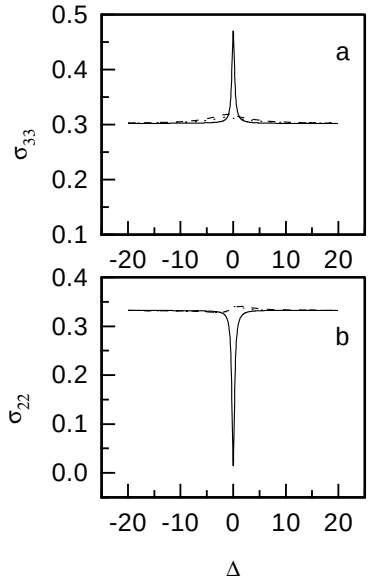

Fig. 4. Same as in Figure 3, but for $N = 10$.

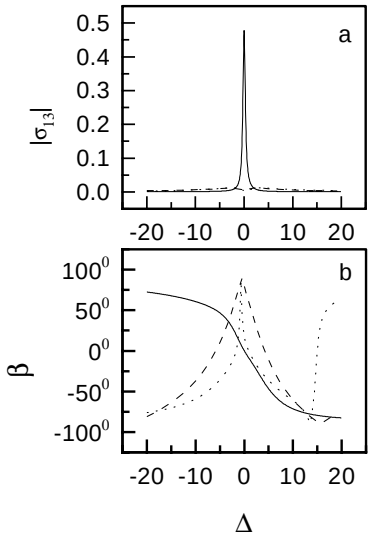

Fig. 5. (a) The modulus of the steady-state two-photon coherence σ_{13} *versus* two-photon detuning Δ. (b) The argument β of σ_{13} *versus* two-photon detuning Δ. Parameter values: $N = 10$, $|M|^2 = N(N+1)$, $\delta = 5$, $\xi_1 = \xi_2 = \xi = 2$, $\gamma_1 = \gamma_2 = \gamma_{21} = 0.5$, and different Φ: 0 (solid line), $\frac{\pi}{2}$ (dashed line), π (dotted line).

(downward) spike at $\Delta = 0$ for $\Phi = 0$, while no such spikes are observed for $\Phi = \frac{\pi}{2}$ or π. The spikes come form the M dependent terms $\frac{1}{2}\gamma_{21}|M|(\sigma_{13}\exp(-i\Phi) + \sigma_{31}\exp(i\Phi))$ in equation (14). When $\Phi = 0$, the two-photon coherence ρ_{13} (ρ_{31}) at $\Delta = 0$ oscillates in phase with the squeezed vacuum (compare Fig. 5), so that a strong exchange of photon pairs of frequency ω_λ and ω_μ, with $\omega_\mu + \omega_\lambda = 2\omega_s$, between the atom and the squeezed vacuum results. As the exchange of photon pairs is accomplished in a single step, the population σ_{22} is extremely low. When $\Phi \neq 0$, the rate of exchange of photon pairs is greatly diminished and the population in the intermediate state σ_{22} is considerable. For $N = 10$, the spikes appear sharper, as shown in Figure 4. Figure 5 exhibits the modulus $|\sigma_{13}|$ and the argument β of the two-photon coherence σ_{13}.

4 Summary

In this paper, we have investigated the steady-state populations of a three-level atom in a ladder configuration, driven by a superposition of an external coherent field with a single broad-band squeezed vacuum. With use of the Born-Markoff approximation, we derive the master equation for the system and obtained the atomic Bloch equations. In general, the coefficients of the Bloch equations are time-dependent. We examine only the case when the carrier frequency of the squeezed vacuum is equal to the frequency of the driving field. For this case, the coefficients of the Bloch equations become time-independent. The steady-state populations can be calculated numerically and shown graphically as functions of two-photon detuning for various cases of the squeezed vacuum.

For the special case of an ordinary vacuum, the populations of the intermediate state shows a resonance at zero lower transition detuning (one-photon absorption), and that of the upper state shows resonances at zero two-photon detuning (two-photon absorption) and at zero lower transition detuning (stepwise excitation) for a weak driving field. For a driving field of intermediate strength, the populations of the intermediate state shows in addition a resonance at zero two-photon detuning, indicating spontaneous emission from the upper level following the resonant two-photon absorption.

For the case of a thermal-like reservoir, the populations show a background determined by the Boltzmann distribution. When the average number of photons per mode in the reservoir is not too large, besides the resonances already discussed, the population of the intermediate state exhibits a dip and that of the upper state a hill at zero upper transition detuning, indicating a one-photon transition. If the average number of photons per mode in the reservoir is sufficiently large, the effect of driving field will be overwhelmed. Only the background population is displayed.

For the case of a squeezed vacuum in minimum uncertainty state, in addition to the resonances already discussed, the population of the upper (intermediate) state shows an upward (downward) spike at zero two-photon detuning under the condition of phase matching, indicating absorption of quantum correlated photon pairs from the squeezed vacuum. No such spikes are observed if the phase matching condition is not fulfilled.

The work is supported by the National Natural Science Foundation of China and Doctral Foundation of the Chinese Education Committee.

References

1. H.J. Kimble, D.F. Wall, J. Opt. Soc. Am. B **4** (10), special issue (1987); R. Loudon, P.L. Knight, J. Mod. Optics, **34** (6/7), special issue (1987).
2. C.W. Gardiner, Phys. Rev. Lett. **56**, 1917 (1986).
3. H.J. Carmichael, A.S. Lane, D.F. Walls, J. Mod. Optics **34**, 821 (1987).
4. H. Ritsch, P. Zoller, Optics Commun. **64**, 523 (1987).
5. Z. Ficek, B.J. Dalton, Optics Commun. **102**, 231 (1993).
6. G.J. Milburn, Phys. Rev. A **34**, 4882 (1986); G.M. Palma, P.L. Knight, Optics Commun. **73**, 131 (1989); Z. Ficek, J. Mod. Optics **40**, 2333 (1993).
7. S. Smart, S. Swain, Phys. Rev. A **48**, R50 (1993); S. Swain, Phys. Rev. Lett. **73**, 1493 (1994); S. Swain, P. Zhou, Phys. Rev. A **52**, 4845 (1995).
8. Z. Ficek, W.S. Smyth, S. Swain, Optics Commun. **110**, 555 (1994); Phys. Rev. A **52**, 4126 (1995).
9. A.S. Parkins, Phys. Rev. A **42**, 4352, 6873 (1990); J.I. Cirac, L.L. Sanchez-Soto, Phys. Rev. A **44**, 1948 (1991).
10. Z. Ficek, P.D. Drummond, Phys. Rev. A **43**, 6247, 6258 (1991).
11. V. Buzek, P.L. Knight, I.K. Kudrayavtsev, Phys. Rev. A **44**, 1931 (1991).
12. Z. Ficek, P.D. Drummond, Europhys. Lett. **24**, 455 (1993).
13. M.R. Ferguson, Z. Ficek, B.J. Dalton, J. Mod. Optics **42**, 679 (1995).
14. M.R. Ferguson, Z. Ficek, B.J. Dalton, Phys. Rev. A **54**, 2379 (1996).
15. B.N. Jagatap, Q.V. Lawande, S.V. Lawande, Phys. Rev. A **43**, 535 (1991).
16. A. Joshi, R.R. Puri, Phys. Rev. A **45**, 2025 (1992).
17. J. Gea-Banacloche, Phys. Rev. Lett. **62**, 1603 (1989); J. Javanainen, P.L. Gould, Phys. Rev. A **41**, 5088 (1990).
18. B.R. Mollow, Phys. Rev. **175**, 1555 (1968).
19. N.Ph. Georgiades, E.S. Polzik, K. Edamastu, H.J. Kimble, A.S. Parkins, Phys. Rev. Lett. **75**, 3426 (1995).
20. A.S. Parkins, C.V. Gardiner, Phys. Rev. A **40**, 3796 (1989); J.I. Cirac, Phys. Rev. A **46**, 4354 (1992).
21. P. Zhou, S. Swain, Phys. Rev. A **54**, 2445 (1996).
22. Z. Ficek, B.J. Dalton, P.L. Knight, Phys. Rev. A **51**, 4062 (1995).
23. W.H. Louisell, *Quantum Statistical Properties of Radiation* (Wiley, New York, 1973).
24. D.F. Walls, G.J. Milburn, *Quantum Optics* (Springer-Verlag, 1995).